The Canonical Seyfert Spectrum: The Implications of OSSE Observations

W.N. Johnson, J.E. Grove, R.L. Kinzer, R.A. Kroeger, J.D. Kurfess, and M.S. Strickman
E.O. Hulburt Center for Space Research, Naval Research Laboratory, Washington DC 20375

K. McNaron-Brown
George Mason University, Fairfax VA 22030

D.A. Grabelsky, W.R. Purcell, M.P. Ulmer
Northwestern University, Evanston IL 60208

G.V. Jung
Universities Space Research Association, Code 7650, Naval Research Lab, Washington DC 20375

ABSTRACT

In its first two years of operation, the Oriented Scintillation Spectrometer Experiment (OSSE) on the *Compton Gamma Ray Observatory (CGRO)* observed 26 active galaxies classified as Seyferts. These objects were selected for their historical X-ray characteristics as identified by HEAO-1, EXOSAT and Ginga and include three of the gamma-ray emitting AGN detected prior to the launch of CGRO. OSSE detects approximately half of these objects at a significance of 5σ or greater. The OSSE observations in the 50 keV – 500 keV range indicate spectra which, on average, are significantly softer than the typical photon power law index, $\alpha \sim 1.7$, observed in x-rays. In the case of NGC 4151, the brightest Seyfert 1 detected by OSSE, a distinctly thermal spectrum is observed during both 1991 and 1993 observations. An average Seyfert AGN spectrum is formed by a weighted summation of the individual observations excluding the brightest detections. This average photon spectrum from 26 observations of 15 AGNs is well described by a simple exponential function with an e-folding energy of 45 keV. We summarize the OSSE observations of Seyfert AGN and present the average spectrum above 50 keV.

INTRODUCTION

In a HEAO–1 study of active galaxies, principally Seyfert 1s, in the 2 – 165 keV energy range, Rothschild et al. (1983) suggested a canonical power law spectral shape with a photon number index $\alpha \sim 1.7$ and with remarkably small dispersion in this index. They also calculated the significance of the Seyfert contribution to the cosmic diffuse background if this canonical power law extends much above $\sim$ 100 keV. At these energies, the spectrum from the sum of unresolved AGN would provide a diffuse flux greater than that which is observed. More recent observations in x-rays with the Ginga satellite (Pounds et al. 1990, Matsuoka et al. 1990) have shown Seyfert spectra which are more complex than the simple picture above. Detection of a hard shoulder above 10 keV and a fluorescent iron emission line in many Seyferts has been interpreted as evidence for a reflected component of an incident power law spectrum from a layer of cold material, presumably an accretion disk. Both thermal and non-thermal models have been proposed to explain the observed characteristics.

Report Documentation Page

Form Approved
OMB No. 0704-0188

1. REPORT DATE	2. REPORT TYPE	3. DATES COVERED
1994		**00-00-1994 to 00-00-1994**

4. TITLE AND SUBTITLE	5a. CONTRACT NUMBER
The Canonical Seyfert Spectrum: The Implications of OSSE Observations	5b. GRANT NUMBER
	5c. PROGRAM ELEMENT NUMBER
6. AUTHOR(S)	5d. PROJECT NUMBER
	5e. TASK NUMBER
	5f. WORK UNIT NUMBER
7. PERFORMING ORGANIZATION NAME(S) AND ADDRESS(ES) **Naval Research Laboratory,E.O. Hulburt Center for Space Research,4555 Overlook Avenue, SW,Washington,DC,20375**	8. PERFORMING ORGANIZATION REPORT NUMBER
9. SPONSORING/MONITORING AGENCY NAME(S) AND ADDRESS(ES)	10. SPONSOR/MONITOR'S ACRONYM(S)
	11. SPONSOR/MONITOR'S REPORT NUMBER(S)

12. DISTRIBUTION/AVAILABILITY STATEMENT
Approved for public release; distribution unlimited

13. SUPPLEMENTARY NOTES

14. ABSTRACT

15. SUBJECT TERMS

16. SECURITY CLASSIFICATION OF:			17. LIMITATION OF ABSTRACT	18. NUMBER OF PAGES	19a. NAME OF RESPONSIBLE PERSON
a. REPORT	b. ABSTRACT	c. THIS PAGE			
unclassified	**unclassified**	**unclassified**		**10**	

Detailed non-thermal models have been developed which make the x-ray and gamma-ray photons by Compton upscattering soft photons by a power law distribution of relativistic electrons. These models include the $e^+ - e^-$ pair production which occurs as the upscattered gamma rays suffer $\gamma - \gamma$ interactions with the lower energy x-ray photons. The creation of these pairs and their subsequent interactions significantly alters the original power law shape (eg. Lightman & Zdziarski 1987). For compact sources with high luminosity, a broad pair annihilation feature at 0.511 MeV is formed. A correlation between luminosity and the observed power law index is also predicted. Coppi & Zdziarski (1992) have successfully applied a nonthermal pair model to observations of the Seyfert galaxy NGC 4151. Their model successfully describes the differing spectral states of the source observed in x-rays and gamma rays by Ginga/HEXE in 1987 (Maisack & Yaqoob 1991) and by the ART-P and SIGMA instruments on GRANAT in 1990 (Apal'kov et al. 1992).

An OSSE observation of NGC 4151 in 1991 (Maisack et al. 1993) measured a spectrum above 50 keV which is similar to the SIGMA spectrum of 1990 but with a sensitivity far exceeding previous observations in this band. Contrary to previous measurements, the OSSE spectrum cannot be described by a single power law. It is best modeled by a broken power law or by exponential shapes such as the thermal Comptonization model of Sunyaev & Titarchuk (1980) with temperatures of ~ 40 keV. This is in marked contrast to the hard spectrum, $\alpha \sim 1.3$, observed by Perotti et al. (1981a) extending to several MeV. In a combined analysis of the 1991 OSSE data on NGC 4151 and the Ginga x-ray data from an observation one month earlier, Zdziarski, Lightman, and Zaciolek-Niedzwiecki (1993) confirm the essentially thermal nature of the spectrum. They proposed a modified non-thermal pair model in which the efficiency of the acceleration of relativistic electrons is $\sim 20\%$. This inefficiency gives rise to a dominant thermal component with a annihilation feature from the non-thermal component. Although a pure non-thermal pair cascade model can be ruled out, a purely thermal explanation can not be.

Thermal models have long been used to describe the x-ray and gamma-ray emission of Cygnus X-1, a suspected black hole source, as well as X-ray emission from AGN. The onset of pair production in these models at temperatures of several hundred keV limits the maximum temperature of the emission region in thermal models to 1 – 2 MeV (Svensson 1984; Dermer 1989). A confirmation by OSSE of the intense gamma radiation extending to 10 MeV, as reported by the MISO experiment for NGC 4151 (Perotti et al. 1981a) and for MCG +8–11–11 (Perotti et al. 1981b) would provide a crucial test for thermal models of AGN.

The OSSE energy band is ideally suited for the study of the importance of non-thermal pair processes because it covers both the band where $\gamma - \gamma$ pair creation is important and the 0.511 MeV pair annihilation feature appears. The combination of x-ray observations and OSSE observations is particularly useful in understanding the emission processes in AGN, as was demonstrated for NGC 4151. OSSE's observations of AGN in the first two years of the *CGRO* mission were designed to measure the gamma ray spectra of AGN with known x-ray characteristics. Seyfert AGN from the HEAO-1 detections (Rothschild et al. 1983) as well as bright objects detected by EXOSAT and Ginga satellites were scheduled for OSSE observations. The objectives of the observations were to improve the spectroscopy into the MeV energy band with hopes of providing insight into emission mechanisms in AGN, the contribution of Seyferts

to the cosmic diffuse background, and the importance of non-thermal processes in Seyferts which might explain the MeV emission reported from two Seyferts, NGC 4151 and MCG+8 − 11 − 11. These non-thermal processes would likely give rise to e^+–e^- pairs which in turn could produce detectable pair annihilation features from these objects.

OBSERVATIONS

OSSE was designed to undertake γ-ray observations of astrophysical sources in the $0.05 - 10$ MeV range. The instrument consists of four identical large-area NaI(Tl)–CsI(Na) phoswich detector systems, each of which is actively shielded by a NaI(Tl) annulus and passively collimated by a tungsten slat collimator that defines a $3.8^\circ \times 11.4^\circ$ full-width at half-maximum (FWHM) γ-ray aperture. Each detector has an independent orientation control system which permits offset-pointed background observations and provides the ability to study two gamma-ray sources per orbit. The total aperture area of the four detectors is 2620 cm^2, with an effective photopeak area of $\sim$ 1900 cm^2 at 100 keV and $\sim$ 2000 cm^2 at 511 keV.

CGRO observations consist of two- to three-week periods of constant attitude during which OSSE generally selects two sources for study, each being observed during a different part of each orbit. Each OSSE observation comprises a sequence of 2-min. observations of a source field alternated with 2-min. offset-pointed background measurements. The 2-min. duration is selected to be short relative to the typical orbital background variations. When possible, source-free fields offset 4.5° on each side of the source position along the detector scan plane are used for background observations. Alternate background offsets can be used to avoid known or suspected gamma-ray sources which would otherwise appear in a background field. The series of background observations is used to estimate the background contribution to each source observation so that the source flux can be extracted. A channel-by-channel prediction of the background spectrum during each two-minute source observation is obtained by interpolation from the neighboring time-sequential series of background measurements. A quadratic fit to three or four nearest (in time) two-minute background intervals is used. Data screening before and after background subtraction insures that only the highest quality difference spectra are combined into the resultant source spectrum. For a typical observation time of 5×10^5 seconds, OSSE generally achieves a sensitivity (3σ) of $\sim 1.2 \times 10^{-3}$ photons cm^{-2} s^{-1} MeV^{-1} in the $50 - 150$ keV band. A more detailed description of OSSE performance and spectral data analysis procedures can be found in Johnson et al. (1993).

During the first two years of the *CGRO* mission, OSSE observed 40 extragalactic objects in $\sim$ 100 separate observations. Of these objects, 17 Seyfert 1 AGN and 9 Seyfert 2 were studied in 59 observations. Table 1 summarizes these Seyfert observations and gives with the detected fluxes from the sources in the $50 - 150$ keV energy band. Upper limits are specified at the 2σ level. Two of the observations were in support of *CGRO* guest investigations; these data were not included in the analyses presented here. As indicated in the table, most of the objects were observed during more than one of the *CGRO* viewing periods. In such cases, the first entry for the source is the weighted average of all the observations. The last column in the table indicates the total live time of quality data on the source position in detector-seconds. A similar time interval was used in background observations associated with the source. As seen

Table 1: OSSE Seyfert Observations

Source[a]	Type	View Period	Date Interval[b]		Flux[c] (50 − 150 keV)	Observ. Time[d]
3C 111	SY 1				2.81 ± 0.49	5.92
		4	91/180	91/193	3.10 ± 0.58	4.33
		29	92/136	92/156	2.06 ± 0.93	1.59
3C 120	SY 1				2.64 ± 0.38	10.01
		29	92/136	92/156	2.13 ± 0.96	1.48
		30	92/156	92/163	< 2.22	1.44
		33	92/184	92/198	3.31 ± 0.77	2.93
		220	93/130	93/133	3.89 ± 1.50	0.57
		224	93/155	93/165	3.21 ± 0.60	3.59
3C 390.3	SY 1				2.68 ± 0.39	10.27
		12	91/291	91/304	4.09 ± 0.69	3.52
		29	92/136	92/156	2.82 ± 0.61	3.62
		209	93/041	93/053	< 1.47	3.12
CEN A	SY 2				50.91 ± 0.43	8.12
		12	91/291	91/304	62.64 ± 0.55	5.70
		43	92/304	92/308	37.73 ± 1.10	1.14
		215	93/092	93/096	31.62 ± 1.39	0.54
		217	93/103	93/110	25.28 ± 1.20	0.74
ESO 141-55	SY 1				< 1.80	2.21
		38	92/240	92/245	3.37 ± 1.23	1.20
		42	92/289	92/303	< 2.62	1.00
IC 4329A	SY 1				5.44 ± 0.61	3.63
		41	92/283	92/289	4.19 ± 1.15	1.04
		44	92/309	92/322	5.92 ± 0.72	2.59
		207	93/013	93/033	GI	3.77
MCG +5-23-16	SY 2				< 2.00	1.32
		36.5	92/226	92/233	< 3.66	0.41
		39	92/246	92/261	< 2.39	0.91
MCG +8-11-11	SY 1				3.68 ± 0.46	7.80
		31	92/163	92/177	4.02 ± 0.51	6.37
		222	93/145	93/151	2.20 ± 1.07	1.43
MCG -5-23-16	SY 2				4.03 ± 0.77	2.87
		35	92/220	92/224	4.60 ± 1.06	1.57
		36	92/224	92/225	< 4.20	0.30
		38	92/241	92/245	4.87 ± 1.33	1.00
MCG -6-30-15	SY 1				4.71 ± 0.61	3.65
		41	92/283	92/289	3.99 ± 1.15	1.05
		44	92/309	92/322	5.00 ± 0.72	2.60
MRK 279	SY 1	22	92/066	92/079	2.56 ± 0.66	3.88
MRK 335	SY 1				< 1.80	2.15
		26	92/115	92/119	< 3.15	0.70
		28	92/129	92/135	< 2.38	1.27
		37	92/234	92/240	< 5.63	0.18

[a] First line/source is total of all observations

[b] Year/Day of Year

[c] $\times 10^{-3} \gamma/\mathrm{cm}^2$-s-MeV, Upper limits are 2σ

[d] $\times 10^5$ Det-secs

Table 1. (cont)

Source[a]	Type	View Period	Date Interval[b]		Flux[c] (50 – 150 keV)	Observ. Time[d]
MRK 509	SY 1				3.99 ± 0.95	1.69
		43	92/304	92/308	4.48 ± 1.36	0.74
		213	93/083	93/088	3.52 ± 1.33	0.94
MRK 841	SY 1	25	92/108	92/114	< 5.27	0.21
NGC 1068	SY 2	21	92/052	92/065	< 1.23	4.52
NGC 1275	SY 2	15	91/333	91/346	1.60 ± 0.57	4.01
NGC 2992	SY 2				< 1.50	3.11
		30	92/157	92/163	< 3.15	0.72
		33	92/185	92/198	< 1.70	2.40
NGC 3783	SY 1	32	92/178	92/184	3.86 ± 1.38	0.94
NGC 4151	SY 1				27.93 ± 0.35	12.01
		4	91/180	91/193	28.58 ± 0.43	7.57
		24	92/094	92/100	24.28 ± 4.06	0.08
		24.5	92/101	92/107	14.87 ± 2.79	0.19
		218	93/111	93/123	25.95 ± 0.75	2.95
		222	93/145	93/151	30.54 ± 1.16	1.23
NGC 4388	SY 2	40	92/262	92/282	6.35 ± 0.58	5.22
NGC 4507	SY 2	208	93/034	93/040	GI	1.44
NGC 4593	SY 1.9				< 1.96	1.41
		36.5	92/229	92/233	< 3.66	0.40
		39	92/258	92/261	< 3.52	0.40
		205	92/365	93/005	< 3.07	0.60
NGC 5548	SY 1.2				3.78 ± 0.74	3.13
		7.5	91/227	91/234	3.34 ± 0.94	1.82
		12	91/291	91/304	4.66 ± 1.81	0.59
		13	91/305	91/311	4.37 ± 1.56	0.73
NGC 6814	SY 1	208	93/034	93/040	3.19 ± 0.83	2.39
NGC 7314	SY 1.9	27	92/120	92/128	< 1.78	1.70
NGC 7582	SY 2				2.57 ± 0.67	3.58
		16	91/347	91/361	2.59 ± 0.81	2.56
		24	92/094	92/100	5.12 ± 1.62	0.54
		24.5	92/101	92/107	< 4.84	0.24
		25	92/108	92/114	< 4.75	0.25

in Table 1, 12 sources were detected at a significance of 4σ or greater; they are, in order of decreasing significance, Cen A, NGC 4151, IC 4329A, NGC 4388, MCG +8–11–11, MCG –6–30–15, 3C 120, 3C 390.3, 3C 111, MCG –5–23–16, NGC 5548 and Mrk 509. OSSE has observed all twelve AGN reported by HEAO-1 (Rothschild et al. 1983) and detects six at 4σ or greater. There is no evidence for emission from the HEAO-1 sources Mrk 335 and ESO 141–55. Cen A has been included in the Seyfert list because of the reported Seyfert 2 characteristics of its nucleus. As a bright radio galaxy it probably belongs in the blazar class of AGN; OSSE's hard spectrum from Cen A also suggests this identification, but Cen A has not been detected by EGRET (Hartman, 1993). Data from Cen A is not included in the following analyses.

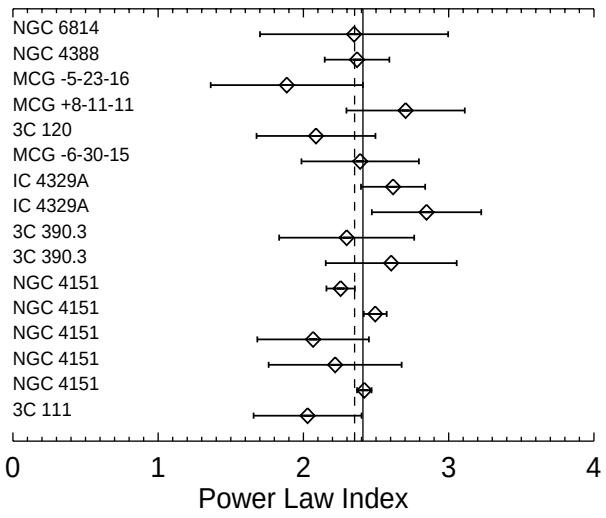

Figure 1: Comparison of best fit power law photon indices for Seyfert observations detection significance of 4σ or greater. Many sources were observed more than once. The horizontal bars represent the 1σ uncertainties in the best fit power law for each observation. The vertical line is the mean index. Variance around the mean is 0.25.

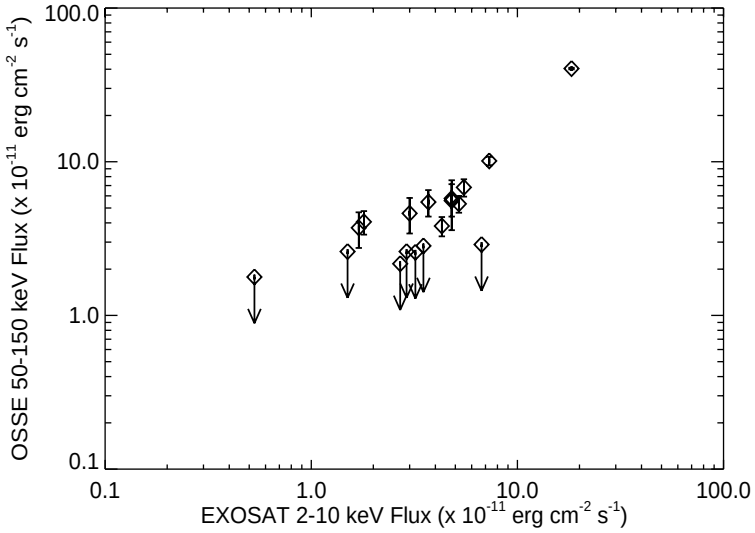

Figure 2: Comparison of historical EXOSAT 2 – 10 keV flux with the OSSE flux in the 50 – 150 keV energy band. OSSE upper limits are plotted at the 2σ level. EXOSAT ME data are from Turner and Pounds (1989).

AVERAGE SEYFERT SPECTRUM

OSSE has observed only one Seyfert AGN, NGC 4151, with sufficient statistical precision to address the thermal vs non-thermal nature of the spectrum above 50 keV. The NGC 4151 spectrum is clearly thermal and, because of its softness and lack of a 0.511 MeV annihilation feature, places fairly restrictive constraint on non-thermal pair models (Maisack et al 1993, Zdziarski et al. 1993). The softening or break in the spectrum of NGC 4151, if assumed to be typical of all AGN, removes the potential excess over the observed cosmic diffuse background and would bring the power law index of the composite AGN spectrum more in line with the diffuse index $\alpha \sim 2.8$ in the 100 – 400 keV band.

The universality of the NGC 4151 spectrum is questioned on the basis of its transitions between type 1 and type 2 Seyfert characteristics (Ayani and Maehara 1991)

and its lack of an apparent reflection component (Maisack and Yaqoob 1991) which is thought to be typical of Seyferts (Pounds et al. 1990). OSSE observations of the bright Seyfert 1, IC 4329A, when combined with Ginga x-ray data appear to be consistent with non-thermal models with a reflection component included (Fabian et al. 1993). In an effort to address the issue of the typical spectrum of Seyfert AGN, the OSSE data from all Seyfert observations with positive detections (here defined as $> 2\sigma$) have been combined to produce an average Seyfert spectrum. The most intense observations ($> 10\sigma$ detections) were excluded so that single sources would not significantly bias the result; this limit removed NGC 4151, NGC 4388 and IC 4329A from the average. The results are not significantly different when NGC 4388 and IC 4329A are included, however. The resultant sum included 26 observations of 15 Seyferts: 3C 111, 3C 120, 3C 390.3, ESO 141–55, MCG +8–11–11, MCG –5–23–16, MCG –6–30–15, Mrk 279, Mrk 509, NGC 1275, NGC 3783, NGC 5548, NGC 6814, NGC 7582.

The individual observations of these sources are well fit by simple power law or exponential models. The statistical precision of the measurements do not permit discrimination between the models. Figure 1 shows the best fit power law indices for the most significant detections ($> 4\sigma$). NGC 4151 and IC 4329A are included in the figure for comparison. The average index for this set is 2.4 with a variance of 0.25 and is clearly softer than the typical power law index, $\alpha \sim 1.7$, in the x-ray band. Figure 2 compares the OSSE flux in the $50 - 150$ keV band to historical fluxes in the $2 - 10$ keV band measured by EXOSAT (Turner and Pounds 1989). The comparison is provided for all sources jointly in the EXOSAT and OSSE observations and include 3C 111, 3C 120, ESO 141–55, IC 4329A, MCG +5–23–16, MCG +8–11–11, MCG –6–30–15, Mrk 335, Mrk 509, NGC 1068 (the weakest), NGC 2992, NGC 3783, NGC 4151 (the brightest), NGC 4593, NGC 5548, NGC 6814, NGC 7314 and NGC 7582.

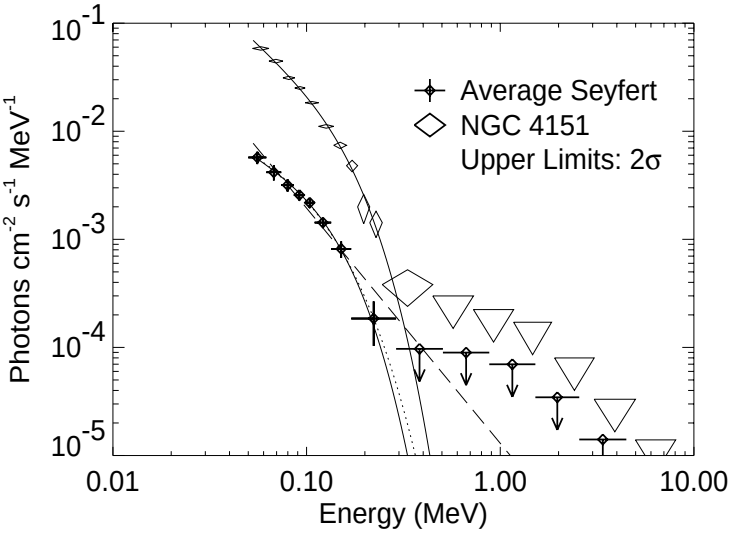

Figure 3: Average OSSE Seyfert Spectrum. Best fit thermal Comptonization (solid line), power law (dashed line) and exponential (dotted line) are shown. The OSSE NGC 4151 spectrum from June, 1991, is shown for comparison with thermal Comptonization fit.

The weighted sum of the 26 OSSE observations of 15 Seyferts is shown in Figure 3. As summarized in Table 2, the spectrum is well described by a simple exponential (solid line in the figure) with e-folding energy of 46 ± 5 keV. The errors given in this table are the 68% confidence limits for joint variation of the respective parameters of interest. Sunyaev-Titarchuk (1980) thermal Comptonization models also provide acceptable fits (dotted line) with kT of $30(+11, -6)$ keV and optical depth of $5.1(+11, -2)$. The best

Table 2: Average OSSE Seyfert Spectral Fits

Exponential:		χ^2 prob. = 0.54
Flux 0.08 MeV	$(4.6 \pm 0.3) \times 10^{-3} \gamma \mathrm{cm}^{-2} \mathrm{s}^{-1} \mathrm{MeV}^{-1}$	
kT	46 ± 5 keV	
Thermal Comptonization:		χ^2 prob. = 0.48
Flux 0.08 MeV	$(4.5 \pm 0.3) \times 10^{-3} \gamma \mathrm{cm}^{-2} \mathrm{s}^{-1} \mathrm{MeV}^{-1}$	
kT	$30(+11, -6)$ keV	
τ	$5.1(+11, -2)$	
Power Law:		χ^2 prob. = 0.06
Flux 0.08 MeV	$(4.2 \pm 0.3) \times 10^{-3} \gamma \mathrm{cm}^{-2} \mathrm{s}^{-1} \mathrm{MeV}^{-1}$	
Photon Index	2.20 ± 0.15	

fit power law model has an index, α, of 2.20 ± 0.15. However the power law model is only a marginally acceptable description of the data with a χ^2 probability of 0.06. Figure 3 shows for comparison the OSSE spectrum of NGC 4151 from the June, 1991, observation. The best fit thermal Comptonization model for NGC 4151 indicated kT of 35 ± 4 keV and τ of 3.4 ± 0.6. (These values differ slightly from those in Maisack et al. 1993 because of an improved calibration of the OSSE instrument response.)

DISCUSSION

The OSSE observations of Seyfert AGN indicate spectra above 50 keV which are softer than the power law with photon index 1.7 which generally describes the Seyfert x-ray spectrum below 50 keV. The best fit power law to the average OSSE data, while not a particularly good description of the data, has an index of 2.2. Thermal models provide better parameterization of the softening or break in the OSSE spectra which occurs around 100 keV or above. This softening or break is not theoretically unexpected or unwelcome. As discussed by Rothschild et al. (1983), the sum of the assumed canonical x-ray power laws ($\alpha \sim 1.7$) from unresolved AGN would provide a diffuse flux greater than that observed at energies above a few hundred keV. The softening observed by OSSE removes this potential excess and suggests that the composite AGN spectrum could be more in line with the observed diffuse background power law, $\alpha \sim$ 2.8, in the $100 - 500$ keV band (e.g. Gruber et al. 1985).

While it is important to obtain good x-ray spectra to compare with the OSSE average Seyfert spectrum, the preliminary indication from the OSSE data alone is that non-thermal pair processes may not be as important as originally believed. It appears that Seyferts have soft or thermal spectra and that the blazar-type AGN are the only ones which exhibit hard emission extending into the GeV range (Fichtel et al. 1993, McNaron-Brown et al. 1993, Dermer 1993). OSSE has seen no MeV emission similar to the balloon observations of NGC 4151 and MCG +8–11–11. Such emission extending

to several MeV would create serious problems for thermal models of emission.

To obtain a spectrum as soft as that obtained by OSSE for the average Seyfert, non-thermal pair models are driven to postulate photon starved pair plasmas where the number of soft seed photons is much less than the number of upscattered photons (Zdziarski et al. 1993). This produces an x-ray spectrum much harder than generally observed and leaves a significant fraction of the energy in thermal pairs. These thermal pairs can give rise to detectable 0.511 pair annihilation radiation. OSSE has seen no indication of broad pair annihilation emission from any of the Seyferts; the OSSE limits on such annihilation features, as a percentage of total source luminosity, may only be interesting for the brightest Seyfert, NGC 4151.

ACKNOWLEDGMENTS

This work was supported under NASA grant DPR S-10987C.

REFERENCES

Ayani, K. and Machara, M. 1991 Publ. Astr. Soc. Japan, 43, L1

Apal'kov, Y., Babalyan, G., Dekhanov, I., Grebenev, S., Lagunov, I., Pavlinskiy, M. and Sunyaev, R. 1992, in Frontiers of X-Ray Astronomy, ed. Y. Tanaka and K. Koyama (Tokyo: Universal Academy Press), 251

Bassani, L. and Dean, A.J. 1983, Spa. Sci. Rev., 35,367

Coppi, P. S. and Zdziarski, A. A. 1992, ApJ, 398, L37

Dermer, C. D. 1989, in Proc. 14th Texas Symposium on Relativistic Astrophysics, ed. E. Fenyves (New York Academy of Sciences, New York), p. 513

Dermer, C. D. 1993, AIP Conference Proceedings, 280, 541

Fabian, A., et al. 1993, ApJ in press.

Fichtel, C.E. et al. 1993, AIP Conference Proceedings, 280, 461.

Gruber, D. E., Matteson, J. L., Jung, G. V. and Kinzer, R. L. 1985, in Proceedings of 19th ICRC, LaJolla CA, OG Vol. 1, 349

Hartman, R.C. 1993, private communicaton

Johnson, W.N. et al. 1992, ApJS, **86**, 693

Jourdain, E. et al. 1992, A&A, 256, L38

Lightman, A. P. and Zdziarski,A. A. 1987, ApJ, 319, 643

Maisack, M., et al. 1993, ApJL, 407, L67

Maisack, M. and Yaqoob, T. 1991, A&A, 249,25

Matsuoka, M. Piro, L., Yamauchi, M., Murakami, T., 1990. ApJ, 361, 440

McNaron-Brown, K. et al. 1993, this volume

Perotti, F., Della Ventura, A., Villa, G., Bassani, L., Butler, R. C., Carter, J. N., Dean, A. J. 1981a ApJ, 247, L63

Perotti, F. et al. 1981b, Nature, 292, 133.

Perotti, F. et al. 1990, A&A, 234, 106.

Pounds, K.A., Nandra, K., Stewart, G.C., George, I.M., Fabian, A.C., 1990. Nat, 344, 132

Rothschild, R. E., Mushotzky, R. F., Baity, W. A., Gruber, D. E., Matteson, J. L. and Peterson, L. E. 1983, ApJ, 269, 423

Sunyaev, R. A. and Titarchuk, L. G. 1980, A&A, 86,121

Svensson, R. 1984, MNRAS, 209, 175

Turner, T.J. and Pounds, K.A. 1989, MNRAS, 240, 833

Zdziarski, A.A., Lightman, A.P. and Maciolek-Niedzwiecki, A. 1993, ApJL, 414, L93